INTRODUCTION

Cardiovascular disease is the number one cause of death worldwide, contributing nearly a third of deaths annually (World Health Organization, 2017). The ability to non invasively diagnose cardiac conditions using tools such as electrocardiogram (ECG) (Gould et al., 1980) and echocardiogram (EOG) forms an essential component of diagnosis and care. Despite their important and longstanding use in diagnosing cardiovascular conditions, non invasive measurements of the electrical activity of the heart still have existing challenges. Much of the interpretation of readings relies on the 'art' of the professional doing the diagnosis, despite standardization and attempts at quantification (Poulikakos and Malik, 2016). Part of the reason interpretation remains so subjective, is that electrical recordings of the heart often experience significant artifacts, noise, and inconsistencies from beat to beat (Pérez-Riera et al., 2017). The inconsistencies come from a variety of factors such as the movement or position of the patient, hemodynamic factors, or the patient's individual physiology (Nguyen et al., 2015). All have an especially notable impact in instances concerned with 'serial ECG comparison', such as during patient monitoring, scientific studies, or drug tests (Zywietz et al., 2003). In an effort to address some of these existing issues, our approach is to offer an additional method for quantifying non-invasively measured electrical signals of the heart. By using topological data analysis, we are able to characterize conduction disturbances in an alternative manner.

BACKGROUND

In this section we offer a basic primer on non invasive tools for measuring the electrical activity of the heart. We also cover the electrophysiology of the cardiac cycle, the bundle branches, and current ECG interpretation guidelines. Finally, we include a brief introduction on topological data analysis and persistent homology.

Electrocardiogram and Vectorcardiogram

Electrocardiograms measure the electrical activity of the heart throughout the cardiac cycle. Electrodes are placed on the patient in order to measure the electrical potential of the heart at several different angles. The voltage readings from these leads are plotted to show the magnitude and direction of muscle depolarization over the course of time. The ECG lets us examine how the cardiac cycle is operating continuously in time. An ECG reading comprises three sections which derive from the physiology of the heart. The P wave, the QRS complex, and the T wave. These three sections correspond to a cycle of depolarization occurring in different regions of the heart. In this paper, we will investigate a novel method for characterizing the PQRST complex of bundle branch block, derived from ECG signal data. A

vectorcardiogram (VCG) is a three-dimensional representation of cardiac activity where the magnitude and direction of the electrical forces of the heart are represented by vectors. A continuous series of positive vectors represent the start of depolarization in the ventricles. As the depolarization spreads through the endocardial surfaces, the vectors grow in magnitude. The vectors change direction with the depolarization as it moves through the heart from left to right and vanish as the depolarization ends. Vectorcardiograms can be produced using three orthogonal leads, or alternatively by transforming ECG data.

Cardiac Electrical Conduction System

The heart's pumping mechanism is managed through the electrical conduction system. Starting at the sinoatrial node, an electrical impulse is generated which travels to the atrioventricular node where it is delayed in order to ensure blood has been ejected from the atria to the ventricles. The electrical impulse then moves to the bundle of His and on down to the Purkinje fibers which allow the ventricles to contract.

Bundle Branch Block

Bundle branches form part of the electrical conduction system of the heart. They are responsible for carrying cardiac action potentials from the bundle of His to the Purkinje fibers. The left bundle branch activates the left ventricle and the right bundle branch, the right ventricle. Injury to the bundle branches can occur from coronary artery disease, valve disease, myocardial infarction or from a variety of cardiac conditions (Bundle Branch Block, n.d.). As such, if the bundle branches are unable to function correctly, then ventricular depolarization may be interrupted. If this occurs, the electrical impulse that would normally travel down the bundle branches is forced through other muscle fibers that are not optimal for the job. Charting a new path through the heart, the electrical impulse is disrupted both in direction, and in speed. Bundle branch block is typically diagnosed from a 12-lead ECG. Bundle branch block in adults is identifiable based on several characteristics (Surawicz et al., 2009):

Figure 1. ECg Recordings from a healthy control (A), and from a patient with left bundle branch block (B). AHA Diagnostic criteria: Left bundle branch block (LBBB): 1. QRS duration greater than or equal to 120 ms 2. Broad notched or slurred R wave in leads I, aVL, V5, and V6and an occasional RS pattern in V5and V6attributed to displaced transition of QRS complex. 3. Absent q waves in leads I, V5, and V6, but in the lead aVL, a narrow q wave may be present in the absence of myocardial pathology. 4. R peak time greater than 60 ms in leads V5and V6but normal in leads V1, V2, and V3, when small initial r waves can be discerned in the above leads. 5. ST and T waves usually opposite in direction to QRS. 6. Positive T wave in leads with upright QRS may be normal (positive concordance). 7. The appearance of LBBB may change the mean QRS axis in the frontal plane to the right, to the left, or to a superior, in a rate-dependent manner

Topological Data Analysis

The goal of topological data analysis (TDA) is to apply concepts from algebraic topology to the practice of studying data. Topology is concerned with studying properties that are preserved under continuous deformation. Generally speaking, TDA seeks to understand what the topological 'shape' of the data is, and what that shape can tell us about the properties underlying the data set, such as how the geometric features change when manipulated or deformed. One of the most popular tools for characterizing the shape of data is calculating persistent homology. Persistent homology has been applied to a wide variety of areas.

In genomics, it has been utilized to study very high dimensional data that is noisy due to 'poorly understood system errors'(Rabadan and Blumberg, 2019). Additionally, it has been used to create high resolution, whole genome maps of meiotic recombination for seven human populations (Camara et al., 2016). In that application, the first Betti number was used to identify spaces where recombination events

occurred. The result is that persistent homology can estimate the amount of recombination in a sample.

In time series, applications include attempts to improve the ability of classifiers to work on chaotic time series. By mapping a time series to a three dimensional Euclidean space using a quasi-attractor, then computing persistent homology on the quasi-attractor waveforms, useful features can be produced (Umeda, 2016).

In the realm of image classification, persistent homology has been used to create additional information about images to serve as inputs in deep learning classifiers (Dey et al., 2017). Other work has taken a topological approach to identifying which features are critical in convolutional neural network classifiers. In this instance, TDA was used to identify problematic clusters from a point cloud generated by the final convolutional layer (Broussard, 2018).

Although persistent homology offers a way to examine high dimensional data structures, the difficulty in interpreting or analyzing high dimensional holes has meant that is has been widely used for low dimensional data (Belkin et al., 2007).

Simplices

Let's say our space of study is a set of points in Euclidean space. A simplex is an n-dimensional representation of a triangle, with 0 simplices being points. Start by surrounding each point with a ball of diameter delta. As you increase the size of the diameter, eventually two balls will intersect. When they intersect, connect the two points inside the balls by an edge. This edge is a 1 simplex. Continue increasing delta until three balls intersect, forming a triangle which is a 2-simplex. A 3-simplex is a tetrahedron, a 4-simplex is a 5-cell and so on. So, formally defined,

$\sum_{i=1}^{N} c_i * \sigma_i$ where each c_i is an integer and σ_i is an oriented k-simplex.

If we use that definition, then from a collection of points and a given delta, we have a complex of associated simplices called the Vietoris Rips Complex, or simply the Rips complex. The Rips complex is commonly used primarily as it is much easier to compute than other complexes such as the Cech complex (Zomorodian, 2010). A face of a simplex is a subsimplex generated by a subset of vertices of a simplex.

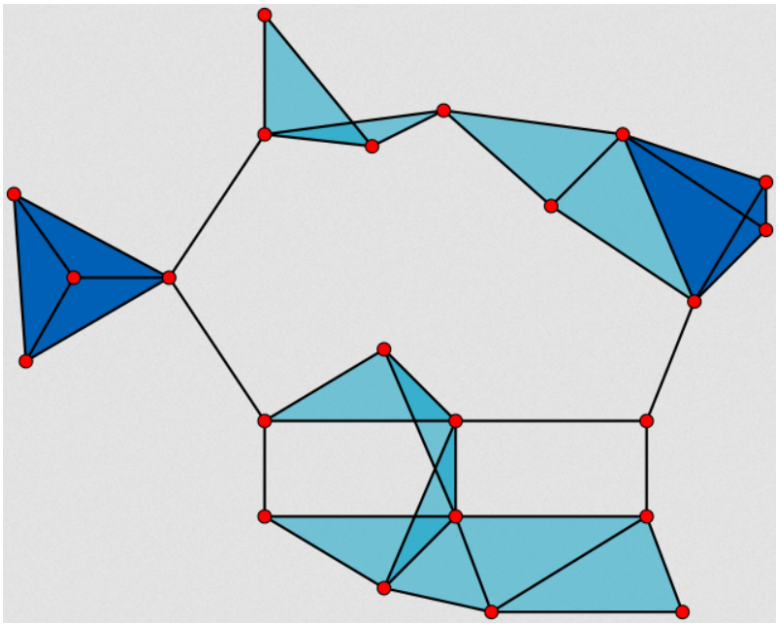

Figure 2. The Vietoris Rips complex on a set of points in R2. Credits to David Eppstein for the image.

Chains

Given a simplicial complex sigma, a k-chain complex associated with the simplicial complex is defined by:

$\sum_{i=1}^{N} c_i * \sigma_i$ where each c_i is an integer and σ_i is an oriented k-simplex.

For our purposes, c_i comes from the field $\mathbb{Z}_2$, meaning that the k-chain is just a collection of k-simplices. A set of k-chains with an associated operator (+) forms a group, C_k.

Boundary Operator

For a k-simplex $\sigma = (v_0 ... v_k)$, the boundary operator $\delta_k : C_k \to C_{k-1}$ is the homomorphism defined by $\delta_k(\sigma) = \sum_{i=0}^{k} (-1)^i (v_0 ... v_i ... v_k)$ where $(v_0 ... v_i ... v_k)$ is the i^{th} face of σ obtained by deleting its i^{th} vertex.

So, for example if we have a 1-simplex $[v_0, v_1]$, then $\delta[v_0, v_1] = [v_1] - [v_0]$. If we have a 2-simplex $[v_0, v_1, v_2]$, then $\delta[v_0, v_1, v_2] = [v_1, v_2] - [v_0, v_2] + [v_0, v_1]$. When we use $\mathbb{Z}_2$, because a-b = b+b, the orientation does not matter, so the boundary of a k-simplex is all of its k-1 simplices. Additionally, for a given k-chain, the boundary is the sum of the boundaries of its simplices.

Cycles, Boundaries, and Homology Group

The k-chain group has a subgroup Z_k, where the elements of Z_k are the kernel of the boundary map, called 'cycles'. The k-chain group also has a subgroup B_k, where the elements of B_k are the image of the k+1

boundary map, called boundaries.

The subgroup of C_k, $Z_k := ker(\delta_k)$ has elements called "cycles" and the subgroup of $C_k, B_k := im(\delta_(k+1))$ has elements called "boundaries".

We define the kth homology group as:

The k^{th} homology goup H_k of S is the quotient group $H_k(S) = Z_k/B_k$. The rank $(H_k(S))$ *is the* k^{th} Betti number of S and gives a count of k-dimensional holes in S.

So, homology groups are equivalence classes of cycles modulo boundaries, in other words they are the independent k-cycles which are not boundaries nor a collection of simplices of the complex, so a hole. The rank of the homology group is the Betti number, and is a count of k-dimensional holes. While the Homology group counts the k-dimensional holes, it only does so for a particular simplicial complex, in this case defined by a particular value for the diameter around the balls used in defining the VR complex. We need a simplicial filtration, and persistent homology in order to study k-dimensional holes at different scales.

Simplicial Filtration and Persistent Homology

Given a simplicial complex S, a filtration of S is a finite sequence of subcomplexes $S^f := S^p | 0 \leq p \leq m$ of S, such that $\emptyset = S_0 \subset S1 \subset ... \subset S_m = S$. For p, q *in* $0...m$ such that $p \leq q$, the persistent k homology group $H_k(S) := Im(i_k)$ where i_k is a linear map between $H_k(S_p)$ *and* $H_k(S_q)$.

So, while the homology finds cycles by factoring out boundaries, the persistent homology identifies cycles that are non boundary elements are one stage of the filtration, that may become boundaries later on. In that way, we can study how cycles persist by looking at what scale they appear, how far along the scale they persist, and at what scale they disappear. These characteristics help us discern what cycles are significant and what we can learn about the shape of the data.

METHODS

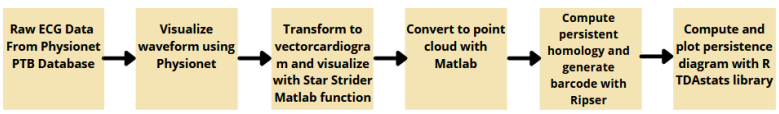

Figure 3. Pipeline for data acquisition, processing, and computation.

In this section we present an overview of our materials and methods including the software packages used for the experiment and visualization.

We began with the Physionet PTB Diagnostic ECG Database (Bousseljot et al., 2009) where we were able to visualize and select high quality ECG recordings to use in our analysis. We selected a high quality reading from a healthy control, from a patient with complete left bundle branch block, and from a patient with complete right bundle branch block. The ECG data was inputted into a MATLAB function for producing vectorcardiograms written for Mathworks File Exchange (Strider, 2014). By taking the initial point for each of the vectors in the vectorcardiogram, a 3-dimensional point cloud representation of the PQRST complex was produced.

Using the Ripser software package (Bauer, 2021), we computed the 0th and 1st dimensional persistent homology for the individual point clouds for each patient using the Vietoris Rips complex. From Ripser, we obtained homology intervals (b,d) for each patient where b is the delta at which the homology first appeared, and d is the delta when it disappeared.

We visualized the lifespans of our features in three ways. The first was to produce a barcode diagram (CARLSSON et al., 2005) where the lifespans are represented by lines on a plot originating at the birth of the feature and ending at its death. The single common axis is the value of delta. The homologies that persist are shown with longer lifespans that continue through increasing delta. Features with very short lifespans are noise in the data or small irregularities on the vectorcardiogram. The second method to visualize the birth death intervals, is the use of a persistence diagram (Edelsbrunner et al.), where the features are plotted according to their birth (x axis) and death (y axis). Features that exist near the diagonal are those with very short lifespans, which are often considered to be noise (Xia and Wei, 2014). Finally, a box plot gives insight into how the birth and death vary by condition for all features.

RESULTS

In this section, we present the persistent homology intervals for our two conditions: healthy control and left bundle branch block. We discuss the significance of the feature intervals, and their relationship to the vectorcardiogram and underlying physiology. We also describe the statistical tests we used, and what kind of alternative information smaller features can tell us.

In examining feature intervals, we are concerned with the scale of features, meaning the diameters at which the features persist, and with the lifespan or a feature, meaning how long the feature persists before being swallowed up in the filtration. Our focus will be on 1-dimensional holes, ‘loops’ or ‘tunnels’.

A large feature is one that exists further along the filtration, where the diameter of the ball around the points is large. For example, features that emerge in the point cloud where the points are farther away

from each other. Small features are found at smaller diameters, these include small independent features, but also features that are akin to roughness or distortion in a larger feature. Short features exist only briefly and do not persist. Longer features are more distinct, which lets them survive longer.

Our healthy control has one large feature, two medium, and a few small features. The shape is characterized as smooth and distinct. This can be seen in the relative lack of short features and in the larger scale of the features. The features tend to be larger which indicates 'fast flowing' vectors such that each vector is farther apart from the next in general. This is associated with more freely moving electrical impulse through the bundle branches. Fewer, larger vectors result in fewer, more spaces out points which result in larger scale features.

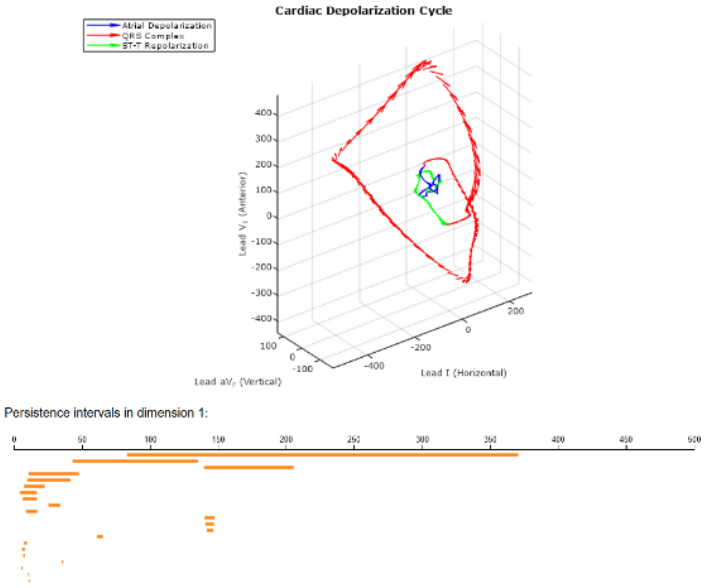

Figure 4. The vectorcardiogram and associated barcode for a healthy control.

The left bundle branch block barcode on the other hand is distinctly different. It has no large features, instead has several medium and many small scale features. In the vectorcardiogram, we can clearly see that the twisted nature of the QRS complex results in rather than having one clearly biggest loop, like in the control, it has been fractured into a number of medium loops that make up the twisted pattern of the vectors. This is indicative of left bundle branch block with underlying congestive heart failure (Pantridge et al., 1950). Additionally, the presence of a large number of smaller and shorter lived features suggests a rougher point cloud, which implies more variation in the speed and direction of the electrical vectors. The greater quantity of small scale disturbances indicates a more muddled flow.

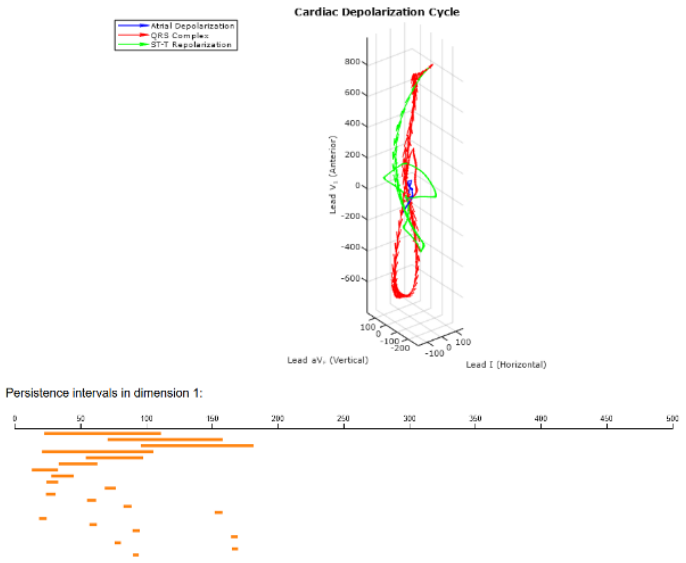

Figure 5. The vectorcardiogram and associated barcode for a patient with LBBB.

If we recall our bundle branch block, the pathology leads to the electrical impulses having to move through less optimal muscle fibers. This manifests itself in the vectorcardiogram by elongated, distorted, non planar QRS complexes (Neuman et al., 1965). These characteristics of shape are preserved in the point cloud and identified by the persistent homology. In essence, persistent homology is a very fine grained characterization of the electrical impulses moving through the heart. When compared to current diagnostic conditions. Such as 120+ QRS and 'broad notched and slurred', persistent homology offers a considerably higher level of detail and a more nuanced description of what is happening. Additionally, the level of detail in persistent homology features are nicely quantified using birth death intervals.

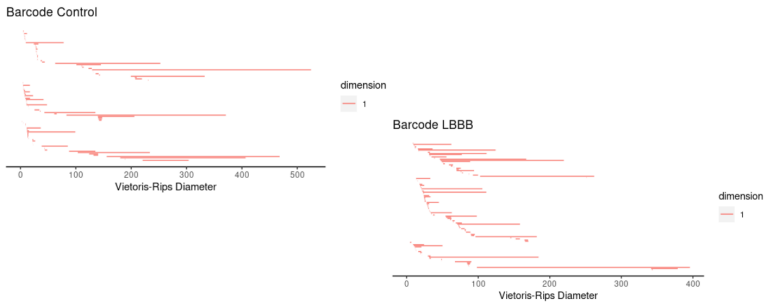

Figure 6. Barcodes for three healthy controls and three individuals with LBBB.

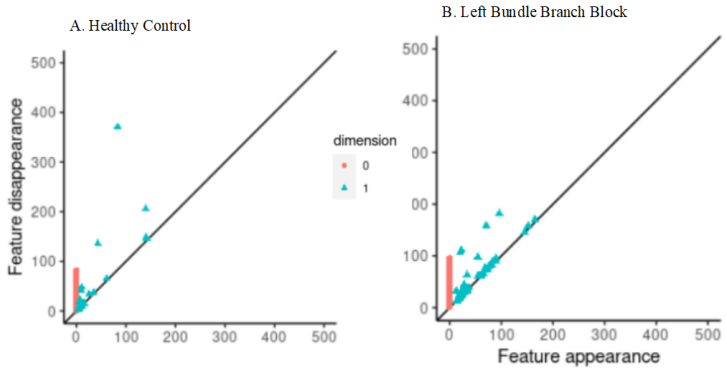

Figure 7. Persistence diagrams for healthy control and LBBB.

To confirm statistically the differences in our sets of birth death intervals, a permutation test between the healthy control and left bundle branch block intervals was conducted using the earth mover's distance. Before the test was performed, 0-dimensional features, very small features, and features with very short lifespans were removed, in order to only test those features which are significant. The test resulted in a p value of 0.04, so we are able to reject the null hypothesis that the birth death intervals come from the same distribution at an alpha of 0.05. In all, our two different conditions produce two distinct barcodes which convey important information about the nature of the PQRST complex during left bundle branch block.

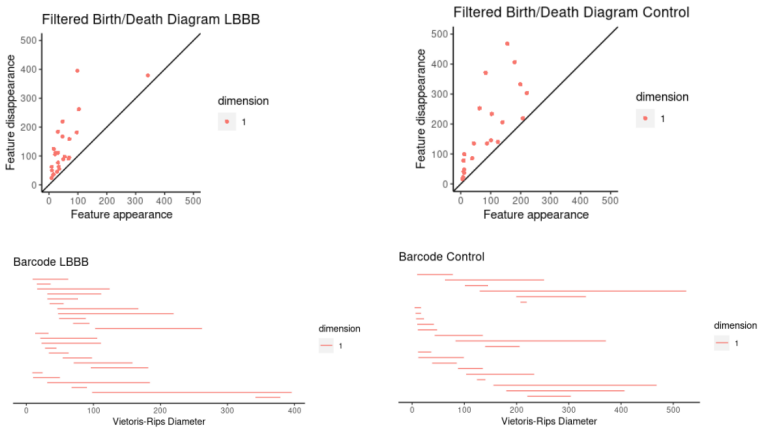

Figure 8. Persistence diagrams and barcodes for filtered feature birth death intervals.

Although we are focused on the more significant features, we can also extract information by looking broadly at trends over all the features including the smaller, noisier ones. This is particularly effective in this context, because the ECG data we used as an input was very high quality with very little noise in the signal. This means that small loops or 'eddies' forming on the edge of the point cloud which are identified by the persistent homology may be an indicator of deformity in the QRS complex. Looking at our historgram, we can see notable differences in births and deaths of features between the different

conditions.

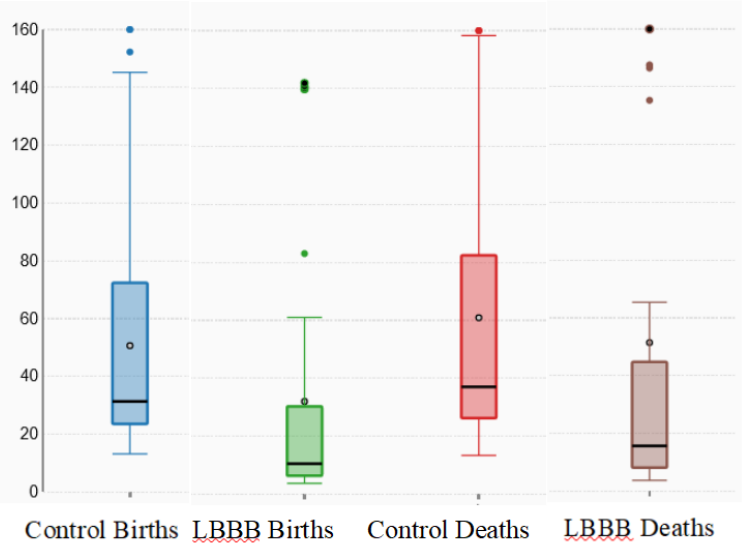

Figure 9. Histogram comparing feature appearance and disappearance for healthy control and LBBB.

DISCUSSION

In this section we discuss the implications of the results, the limitations and challenges with the work, and possible avenues for future work and deeper exploration.

The goal with this method is to be able to quantify bundle branch blocks from ECG data in a way that offers an alternative to traditional means in hopes of improving on some of the existing issues with interpretation and analysis of that data, all while maintaining ease of readability and clear understanding within current paradigms. In particular, persistent homology is useful for quantifying bundle branch blocks in a way that is resistant to beat to beat variation. The reason, is that persistent homologies remain persistent despite perturbations in the QRS loop from one beat to the next. By definition, the homologies persist when the data is disturbed under continuous deformation. Additionally, by quantifying the data using persistent homology intervals, information normally conveyed through three to seven different checklist conditions, is now neatly characterized by an nx2 matrix, where n is the number of features.

Limitations

This work is limited by the fact that persistent homology is still a very new area of study, and methods for statistically analyzing birth death intervals are still largely experimental (Lesnick, 2014). As a result, analysis and interpretation of the barcodes relied heavily on known or expected results from ECGs and VCGs. It is possible that this colored the interpretation of the barcodes and resulted in unintended bias. Additionally, because this paper attempts to offer a new characterization of bundle branch blocks, only very high quality ECG recordings were used, in order to ensure that the data truly represented

the underlying condition under study. 'Bad' data with significant noise and some incorrect labels was also tested and permutation tests resulted in p values between 0.028 and 0.056 which suggests that the persistent homology characterization is still able to differentiate between bundle branch block and healthy controls, but the incorrect labels colored the data too much to use it as a result in the paper.

Future Work

Future work can address this risk of bias in part by trying to remove some of the human interpretation from the equation. Persistent homology intervals have been used extensively as inputs into machine learning classifiers (Adams, 2018). It would be a useful test of the validity of persistent homology on VCG to investigate whether persistent homology intervals are a better data source than raw ECG or VCG data both for accuracy and also for speed of computation. Developments in sheaf theory may also lead to useful advances in being able to distinguish between local and global phenomenon ((Curry, 2014)). Another avenue that may yield interesting results would be to investigate how the persistent homology intervals evolve as a disease progresses. It may be the case that calculating the movement of birth/death point distributions over time can help predict patient outcomes.

ACKNOWLEDGMENTS

Thanks to Dr. Randall Moorman, Dr. Brent French, Dr. Ronald Williams, and Kimberly Fitzhugh-Higgins

REFERENCES

Adams, H. (2018). Survey: From persistent homology to machine learning feature vectors. https://www.math.colostate.ed

Bauer, U. (2021). Ripser: efficient computation of Vietoris–Rips persistence barcodes. Journal of Applied and Computational Topology. https://doi.org/10.1007/s41468-021-00071-5

Belkin, M., Bendich, P., Mukherjee, S., Harer, J. (2007). Geometry and random matrices Persistence homology -theory Persistence homology -(Bayesian) statistical methods Open problems Spring semester extension to High Dimensional Inference and Random Matrices Spring semester extension to High Dimensional Inference and R. https://www2.stat.duke.edu/ sayan/AIM.pdf

Bousseljot, R., Kreiseler, D., Schnabel, A. (2009). Nutzung der EKG-Signaldatenbank CARDIODAT der PTB über das Internet. Biomedizinische Technik/Biomedical Engineering, 317–318. https://doi.org/10.1515/bmte.1995.40.s1.317

Broussard, Matthew. "Exploring Artificial Intelligence through Topological Data Analysis." Washington State University, Sept. 2018, www.math.wsu.edu/faculty/bkrishna/FilesMath592/F18/LecNotes/Broussard$_V GG_S ep2$0

Bundle Branch Block. (n.d.). Texas Heart Institute. https://www.texasheart.org/heart-health/heart-information-center/topics/bundle-branch-block/

Burns, E. (2018, August 1). Right Bundle Branch Block (RBBB) • LITFL • ECG Library Diagnosis. Life in the Fast Lane • LITFL • Medical Blog. https://litfl.com/right-bundle-branch-block-rbbb-ecg-library/

Camara, Pablo G., et al. "Topological Data Analysis Generates High-Resolution, Genome-Wide Maps of Human Recombination." Cell Systems, vol. 3, no. 1, July 2016, pp. 83–94, 10.1016/j.cels.2016.05.008. Accessed 12 Apr. 2020.

CARLSSON, GUNNAR, et al. "PERSISTENCE BARCODES for SHAPES." International Journal of Shape Modeling, vol. 11, no. 02, Dec. 2005, pp. 149–187, 10.1142/s0218654305000761.

Carlsson, Gunnar. "TOPOLOGY and DATA." BULLETIN (New Series) of the AMERICAN MATHEMATICAL SOCIETY, vol. 46, no. 2, 2009, www.ams.org/journals/bull/2009-46-02/S0273-0979-09-01249-X/S0273-0979-09-01249-X.pdf.

Curry, Justin. "Sheaves, Cosheaves and Applications." ArXiv:1303.3255 [Math], 17 Dec. 2014, arxiv.org/abs/1303.3255. Accessed 4 Aug. 2021.

Dey, T., Mandal, S., Varcho, W. (2017). Vision, Modeling, and Visualization (2017) Improved Image Classification using Topological Persistence. https://web.cse.ohio-state.edu/ dey.8/paper/ImagePers/ImagePers.pdf

Edelsbrunner, H., et al. "Topological Persistence and Simplification." Discret. Comput. Geom., 2002, www.semanticscholar.org/paper/Topological-Persistence-and-Simplification-Edelsbrunner- Letscher/cb672955f60bc279
10.1007/s00454-002-2885-2. Accessed 4 Aug. 2021.

Fan, F. (2010). Lecture 8: Introduction to Persistent Homology Topics in Computational Topology: An Algorithmic View. https://web.cse.ohio-state.edu/ wang.1016/courses/788/Lecs/lec8-fengtao.pdf

Gould, L., Reddy, C. V. R., Zen, B., Singh, B. K. (1980). Usefulness of the Electrocardiogram and Vectorcardiogram in Left Bundle Branch Block and Myocardial Infarction. Chest, 77(2), 208–210. https://doi.org/10.1378/chest.77.2.208

Khoury, M. (2010). Lecture 6: Introduction to Simplicial Homology Topics in Computational Topology: An Algorithmic View. https://web.cse.ohio-state.edu/ wang.1016/courses/788/Lecs/lec6-marc.pdf

Lesnick, M. (2014, January 7). Studying the Shape of Data Using Topology - Ideas — Institute for Advanced Study. Www.ias.edu. https://www.ias.edu/ideas/2013/lesnick-topological-data-analysis

Neuman, J., Blackaller, J., Tobin, J. R., Szanto, P. B., Gunnar, R. M. (1965). The spatial vectorcardiogram in left bundle branch block. The American Journal of Cardiology, 16(3), 352–358. https://doi.org/10.1016/0002-9149(65)90726-5

Nguyen, U., Potse, M., Regoli, F., Luce Caputo, M., Conte, G., Murzilli, R., Muzzarelli, S., Moccetti, T., Caiani, E., Prinzen, F., Krause, R., Auricchio, A. (2015). An in-silico analysis of the effect of heart position and orientation on the ECG morphology and vectorcardiogram parameters in patients with heart failure and intraventricular conduction defects. Journal of Electrocardiology, 48(4), 617–625. https://doi.org/10.1016/j.jelectrocard.2015.05.004

PANTRIDGE, J. F., ABILDSKOV, J. A., BURCH, G. E., CRONVICH, J. A. (1950). A Study of the Spatial Vectorcardiogram in Left Bundle Branch Block. Circulation, 1(4), 893–901. https://doi.org/10.1161/01.cir.1.4.893

Pereira, L., Torres, L., Amini, M. (2021). Topological Data Analysis for Network Resilience Quantification. Operations Research Forum, 2(29). https://link.springer.com/article/10.1007/s43069-021-00070-3

Pérez-Riera, A. R., Barbosa-Barros, R., Daminello-Raimundo, R., de Abreu, L. C. (2017). Main artifacts in electrocardiography. Annals of Noninvasive Electrocardiology, 23(2), e12494. https://doi.org/10.1111/anec.12494

Poulikakos, D., Malik, M. (2016). Challenges of ECG monitoring and ECG interpretation in dialysis units. Journal of Electrocardiology, 49(6), 855–859. https://doi.org/10.1016/j.jelectrocard.2016.07.019

Rabadan, R., Blumberg, A. (2019). Topological Data Analysis for Genomics and Evolution.

Strider. (2014, June). Detecting QRS complex in ECG signal - MATLAB Answers - MATLAB Central. Www.mathworks.com. https://www.mathworks.com/matlabcentral/answers/133159-detecting-qrs-complex-in-ecg-signal

Surawicz, B., Childers, R., Deal, B. J., Gettes, L. S. (2009). AHA/ACCF/HRS Recommendations for the Standardization and Interpretation of the Electrocardiogram. Journal of the American College of

Cardiology, 53(11), 976–981. https://doi.org/10.1016/j.jacc.2008.12.013

World Health Organization. (2017). Cardiovascular Diseases (CVDs). Who.int; World Health Organization: WHO. https://www.who.int/news-room/fact-sheets/detail/cardiovascular-diseases-(cvds)

Umeda, Yuhei. "Time Series Classification via Topological Data Analysis." Fujitsu Laboratories LTD, 2016, www.jstage.jst.go.jp/article/tjsai/32/3/32$_D - G72/_p df$.

Xia, K., Wei, G.-W. (2014). Persistent homology analysis of protein structure, flexibility, and folding. International Journal for Numerical Methods in Biomedical Engineering, 30(8), 814–844. https://doi.org/10.1002/cnm.2655

Zhou, Yi. "Persistent Homology on Time Series." Department of Mathematical and Statistical Sciences University of Alberta, 2016, era.library.ualberta.ca/items/9c9b767b-34d7-4aab-b7b0- 4e056303d746/view/8c0ce5d4-58a9-47c9-a38b-ca17cdbbae53/Zhou$_Y i_2$01609$_M Sc - 20.pdf$.

Zomorodian, A. (2010). Fast construction of the Vietoris-Rips complex. Computers Graphics, 34(3), 263–271. https://doi.org/10.1016/j.cag.2010.03.007

Zywietz, C., Widiger, B., Fischer, R. (2003). A System for Comprehensive Comparison of Serial ECG Beats and Serial ECG Recordings. http://cinc.mit.edu/archives/2003/pdf/68